Journal of Polymers and the Environment (2023) 31:3040–3051
https://doi.org/10.1007/s10924-023-02772-7

ORIGINAL PAPER

Synthesis of Carboxyl Cellulose Nanocrystals/Copper Nanohybrids to Endow Waterborne Polyurethane Film with Improved Mechanical and Antibacterial Properties

Xiaoxiao Hu[1] · Yonghuan Zhao[1] · Yang Meng[1] · Chen Shi[1,2] · Jian Han[1,2]

Accepted: 14 January 2023 / Published online: 14 February 2023

Abstract
The multifunctional nanohybrid fillers have attracted widespread attention in the field of polymer nanocomposites. In this study, carboxyl cellulose nanocrystals/copper nanoparticles (TCNC/Cu NP) nanohybrids were prepared by in situ growth of copper ions on the modified carboxyl CNC, and further doped into waterborne polyurethane (WPU) via solution blending. TEM, FTIR, XRD, and UV–vis analysis were used to characterize the morphology, composition, crystallization and structure of the as-prepared nanohybrid. TCNC/Cu NP nanohybrids exhibited good dispersion and interface compatibility in WPU matrix. The nanocomposite film obtained significantly enhanced mechanical, thermal stability and scratch resistance properties, which was attributed to a hydrogen bond network structure formed in the WPU matrix. Additionally, colony count method was performed to test antibacterial properties of various films. Compared to the pure WPU film, all of nanocomposite films showed better antibacterial properties against Escherichia coli and Staphylococcus aureus. The antibacterial ratio of the WPU nanocomposite film with the addition of TCNC/Cu NP (1:1) reach 99%. Furthermore, the results of a copper ion sustained release experiment showed that the nanocomposite film had a long-term release effect, which was ascribed to the strong bonding between TCNC/Cu NP nanohybrids and WPU matrix. Thus, Cu NP was firmly embedded in the hydrogen bonding network structure formed. This work gives a new approach to prepare the antibacterial WPU film with well mechanical properties.

X.X. Hu and Y.H. Zhao contributed equally to this work

✉ Chen Shi
chenshi2021@zstu.edu.cn

✉ Jian Han
jianhan88@sina.cn

[1] College of Materials and Textiles, Zhejiang Sci-Tech University, Hangzhou 310018, People's Republic of China

[2] The Key Lab of Industrial Textile Material and Manufacturing Technology, Zhejiang Province, Hangzhou 310018, People's Republic of China

Graphical Abstract

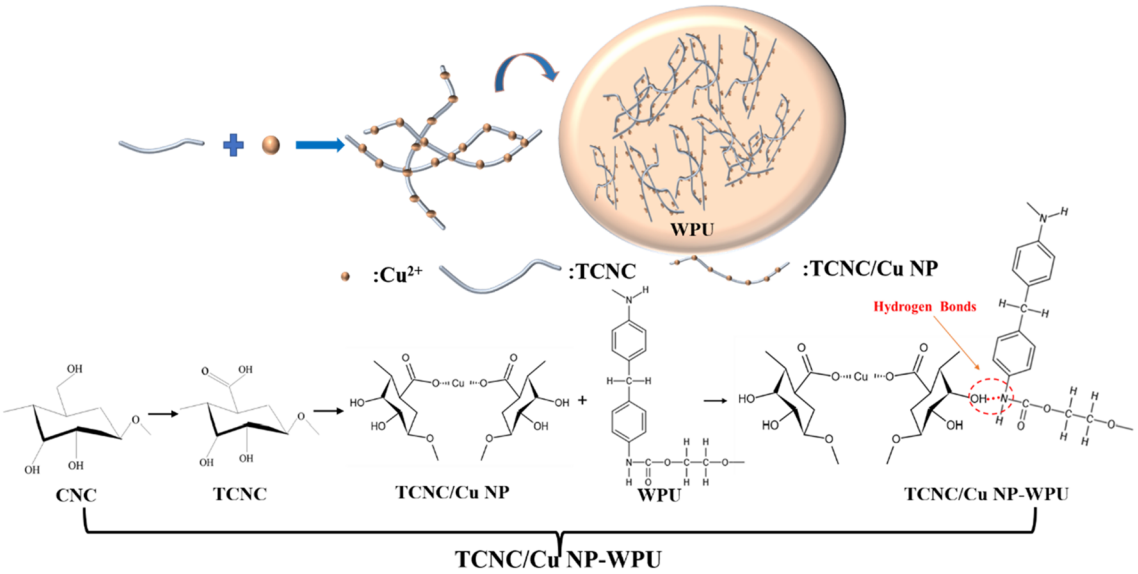

Keywords Cellulose nanocrystals · Copper nanoparticles · Waterborne polyurethane · Antibacterial

Introduction

Waterborne polyurethane (WPU) retains the excellent properties such as low temperature resistance, friction resistance and lower volatile organic compound in comparison with the solvent-based polyurethane [1]. In recent years, WPU has been increasingly used for outdoor textiles such as tents, outdoor protective clothing and other fields [2]. Nevertheless, bacteria can easily grow on the surface of WPU films in a humid environment, which will endanger people's health and sanitary environment [3]. Therefore, it is required to obtain durable and effective antibacterial properties [4]. It is a common and effective strategy for preparation of the antibacterial WPU by adding antibacterial components [5]. At present, the antibacterial agents used for WPU mainly include organic compounds, metal halides, quaternary ammonium salts and so on [6]. Metal-based nanoparticles are widely used because of its high efficiency at a lower dosage [7].

Among them, copper nanoparticle (Cu NP) is regarded to possess great potential application in antibacterial materials, because Cu NP and copper-containing compounds exhibit high-efficiency and broad-spectrum antibacterial activity [8]. The antibacterial mechanism is explained as the contacting of copper ion or releasing of reactive oxygen species [9]. Phana et al. [10] obtained Cu NP with good antibacterial effect, and further explained the antibacterial mechanism. Cu NP can easily enter the interior of bacterial cells through the cell membrane and cause cell death [11]. However, one of the main challenges is how to achieve uniform dispersion and good interfacial bonding of Cu NP in polymers due to the size effect and van der Waals forces of nanoparticles. Nanohybrid composite is considered as a feasible method to disperse Cu NP in the polymer matrix [4]. Meanwhile, the introduction of another component can also reflect a synergistic effect to endow enhanced the performances and more functionality for the polymer matrix. Mirmohsenia et al. [12] prepared copper nanoparticles/reduced single-layer graphene oxide (Cu/rSLGO) nanohybrids by in situ reduction and stabilization of Cu^{2+} ions on SLGO nanosheets, which were added to the WPU dispersions, further obtaining multifunctional antistatic and antibacterial WPU nanocomposite coatings.

Another challenge of the metal nanoparticles-based WPU nanocomposite film is to achieve sustained release of metal ions and long-term antibacterial effect. This requires that the metal nanoparticles have a strong interface with the polymer matrix, so that they can be stably and firmly fixed in the polymer matrix to reduce their migration and detachment from the polymer. Therefore, it is noteworthy to look for a suitable carrier to immobilize copper nanoparticles in the preparation of Cu NP based nanohybrid composites. Recently, cellulose nanocrystal (CNC) has been one of the hottest nanofiller used in polymer nanocomposites. As a rigid rod-shaped nanomaterial with high aspect ratio, it has many advantages such as excellent crystallinity, modulus, strength and biocompatibility [13]. Also, it is often used as

a reinforcing filler for polymers owing to the good dispersion and interfacial compatibility especially in water-based resins. The physical and mechanical properties of the WPU matrix can be improved by adding different forms of nanocellulose [14]. Mondragon et al. [15] isolated CNC from sisal fibers and incorporated it into aqueous WPU to get an aqueous suspension. The modulus of the WPU nanocomposite film with 5% content increased by 100%, the elongation was about 650%, in comparison with the pure WPU film. In addition, CNC is considered as a carrier to directly conjugate metal-based nanoparticles (NP) and highly active metal ions were used as ion-ligand bridges to construct multifunctional nano catalyst as previous work reported [16].

Based on the above considerations, CNC can be used as a carrier for immobilizing copper nanoparticles to synthesize the nanohybrid composite. In this study, carboxyl cellulose nanocrystal (TCNC) was prepared by 2,2,6,6-Tetramethylpiperidine-1-oxyl (TEMPO) oxidation, which can selectively oxidize primary hydroxyl groups on the surface of CNC to carboxyl groups. Then, Cu NP was grown in situ on the surface of TCNC to obtain TCNC/Cu NP nanohybrids. Next, the obtained TCNC/Cu NP nanohybrids were added to aqueous polyurethane dispersion (WPU) and the nanocomposite film was fabricated by casting. The structure, morphology, thermal stability, mechanical properties and antibacterial properties of the final WPU nanocomposite films were characterized. The membrane material in this paper is mainly used for outdoor supplies, such as tents, outdoor protective clothing and so on.

Experiment

Materials

WPU was purchased from Jining Hua kai Resin Co., Ltd.; (solid content 35%, polyester typ.) Microcrystalline cellulose (MCC) was provided by Maclean Co., Ltd.; 2,2,6,6-Tetramethylpiperidine 1-oxyl (TEMPO), sodium bromide (NaBr), sodium hypochlorite (NaClO, 5%), copper chloride ($CuCl_2$), sodium citrate ($C_6H_5Na_3O_7$), ascorbic acid ($C_6H_8O_6$) and sodium hydroxide (NaOH) were supplied by Hangzhou Mike chemical Co., Ltd.; Escherichia coli (E.coli) and Staphylococcus aureus (*S. aureus*) were provided by Shanghai Luwei Technology Co., Ltd.

Surface Modification of CNC

CNC was obtained by acid hydrolysis of MCC as previous work [17]. CNC was modified by NaClO/NaBr/TEMPO oxidation system [18]. First, 0.2 g of CNC was dissolved in 50 mL of water to form a CNC suspension, and 80 mg of sodium bromide (NaBr) was added to the above suspension to form solution A with ultrasonic stirring for 10 min. Then 140 mg of TEMPO was added to 10 mL of water to form solution B. Then mixed solution A with solution B together under stirring for 30 min. Finally, in order to keep the pH at 10.5, NaClO solution and NaOH solution were dropwise added simultaneously. The reaction was sustained for a certain period of time and terminated with ethanol. After washing with deionized water and ethanol in turn several times, the final product carboxylated cellulose nanocrystals (TCNC) was obtained through freeze-dried.

Synthesis of TCNC/Cu NP Nanohybrids

In a typical preparation, 1 mL of aqueous $CuCl_2$ (10 mL, 0.01 M) was added to the TCNC suspension (1 g, 1 wt%), followed by 30 min of stirring. The mixture was heated to 95 °C, 0.025 g of sodium citrate and 10 mL of ascorbic acid (10 mL, 0.01 M) were added in sequence. Finally, 10 mL of sodium hydroxide solution (10 ml, 0.05 M) was added with a dropping funnel. The reaction was continued for 1.5 h until the solution turned reddish-brown. The reactants were centrifuged and washed at 14,000 rpm for 10 min and freeze-dried for 24 h to obtain TCNC/Cu NP. Under the same conditions, while keeping the quality of TCNC unchanged, the amount of $CuCl_2$ was changed to obtain nanohybrid composites with different mass ratios, namely TCNC/Cu NP (1:0.5), TCNC/Cu NP (1:1), TCNC /Cu NP (1:2).

Preparation of TCNC/Cu NP-WPU Nanocomposite Films

TCNC/Cu NP-WPU nanocomposite films were prepared by the solution blending method. First, the as-prepared TCNC/Cu NP (1:0.5), TCNC/Cu NP (1:1) and TCNC/Cu NP (1:2) were dissolved in deionized water to form a dispersion liquid, then added to the WPU matrix. After that, the dispersion is stirred by ultrasonic wave for 1 h, and then poured into the mold. The TCNC/Cu NP WPU film was stand at room temperature for 8 h, and then dried in an oven at 80 °C. These samples are denoted as TCNC/Cu NP (1:0.5)-WPU, TCNC/Cu NP (1:1)-WPU and TCNC/Cu NP (1:2)-WPU. The preparation process is shown in Fig. 1.

Characterization

The molecular composition of TCNC and TCNC/Cu NP sample were determined by Fourier transform infrared spectroscopy (FTIR, 5770, Nicolet). The wavelength range surveyed was 4000–500 cm^{-1} at a resolution of 4 cm^{-1}, and it was done 32 times. The morphology of samples was observed with a JEM-2100 transmission electron microscope (TEM) at an operating voltage of 200 kV. Sedimentation experiments were performed to characterize the

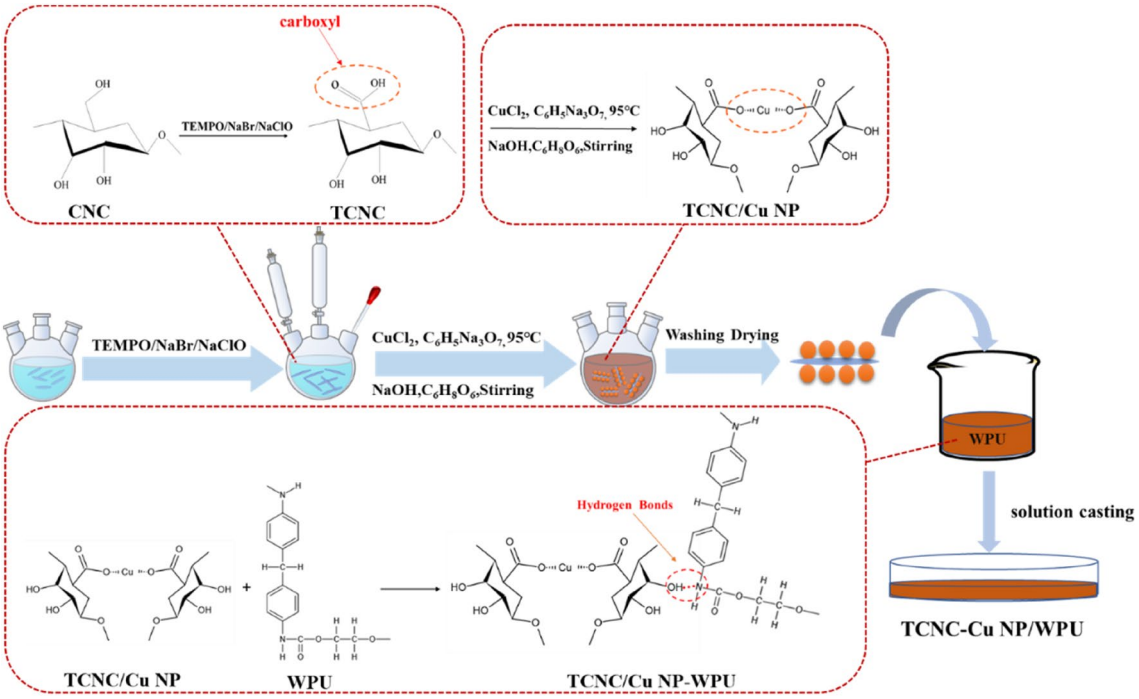

Fig. 1 Schematic diagram of the synthesis process of TCNC/Cu NP-WPU

dispersibility of nanoparticles in water. The sedimentation of various dispersion solution (0.5 wt%) was recorded after settling for 2 h. The crystal structure of TCNC/Cu NP composites was investigated using X-ray diffractometer (XRD, D8 DISCOVERY, Bruker AXS). The scanning range was 10°–80°, 40 kV, 200 mA, and the scanning speed was 5°/min.

Scanning electron microscope (SEM, Ultra55 Zeiss) was used to observe the cross-section morphology of films. The scanning voltage was 5.0 kV. An ultraviolet–visible (UV–Vis) spectrophotometer (UV2600, Shimadzu) with integrated balls was used to measure the UV–Vis spectra in the wavelength range of 300–800 nm. The sample background material was barium sulfate. The surface characteristic of the films was examined by atomic force microscope (AFM) (Bruker Dimension Icon of Germany). Pencil hardness measures the scratch resistance of the coating film to pencils of different hardness. Pencil hardness was measured with QHQ-A pencil hardness tester (Aipu Measuring Instrument Co., Ltd.). The tested angle between the pencil and the test piece was set at 45° to draw about 1 cm in front of the tester. The scraping speed was 1 cm/s, and the pressure of the durometer body on the pencil lead was kept at 1 ± 0.05 kg. The mechanical properties of the nanocomposite films were determined at room temperature using an Instron 3369 universal material testing machine. The size of the samples was 30 mm × 25 mm, and the thickness is about 0.25–0.3 mm. The stretching speed was 100 mm/min. The thermal stability of the WPU film and TCNC/Cu NP-WPU films was determined using a thermogravimetric analyzer (TG, PYRIS 1, Perkin Elmer, USA). The samples were tested in a nitrogen atmosphere with a temperature range of 30–700 °C and a heating rate of 10 °C/min.

0.1 g TCNC/Cu NP (1:1)-WPU composites were put into a volumetric bottle. Then fix the volume to 100 mL with PBS solution. Then put it in a pot with a temperature of 30 ℃. After 24, 48, 72, 96, 120 and 144 h, 10 mL of the solution was taken. The inductively coupled plasma emission spectrometer (Agilent 720ES(OES)) was used to test the sample solution. Each sample was measured three times and the average value was obtained to calculate the copper ion concentration of each sample [23].

The antibacterial activities of the films against *S. aureus* and *E. coli* were detected by bacterial count method. Various bacterial solutions were diluted to 10^2 and 100 µL of the diluted treated and pure film were spread evenly on Luria–Bertani (LB) agar plates. The antibacterial effect of these samples can be observed by the colony count after 24 h. The antimicrobial reduction is obtained according to Eq. (1):

$$\text{Reduction of bacteria (\%)} = (A - B)/A \times 100 \quad (1)$$

where A and B are the number of bacteria on the pure film and treated film after 24 h, respectively.

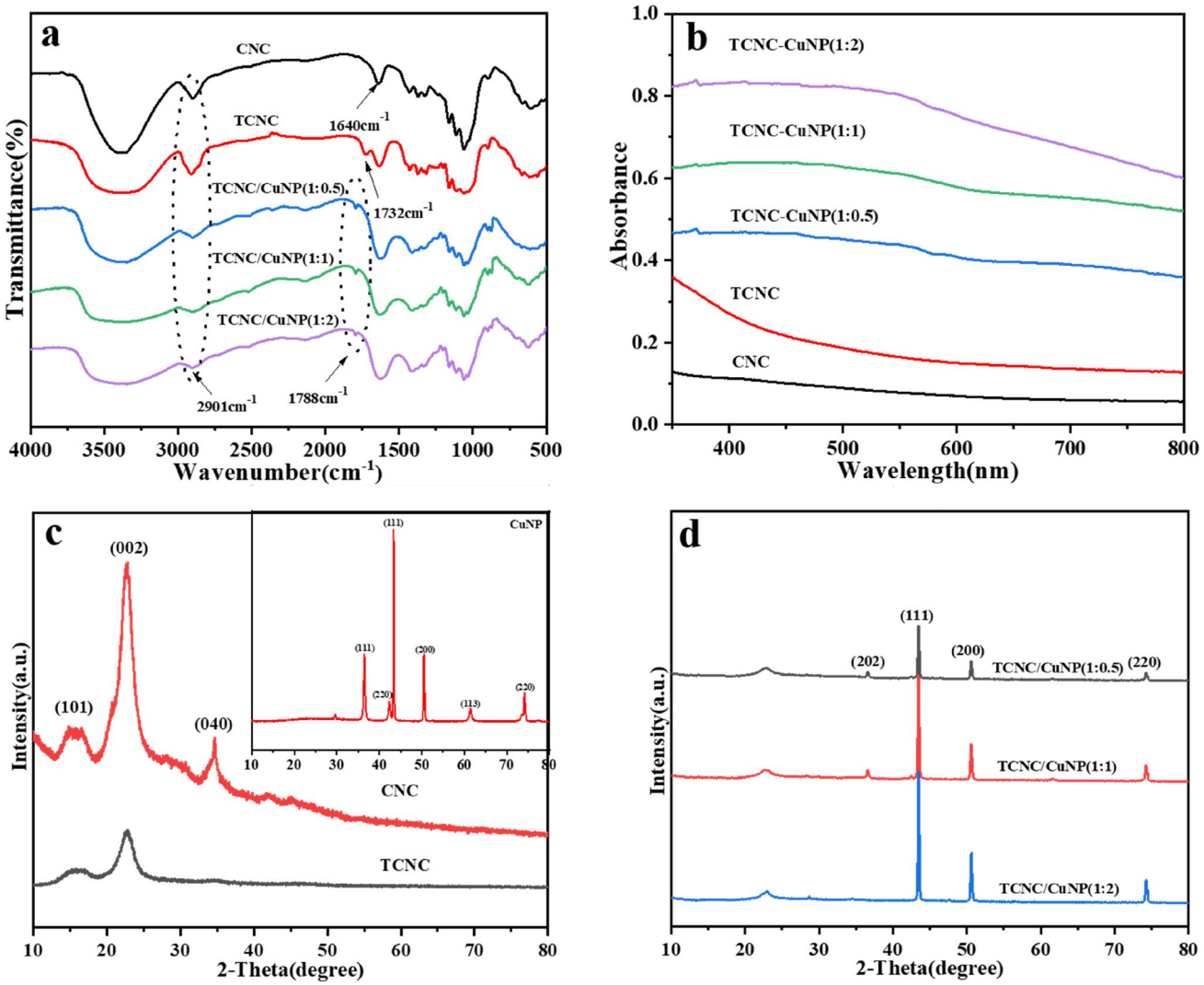

Fig. 2 FTIR spectra of CNC, TCNC, TCNC/Cu NP (**a**) and UV–vis spectra of CNC, TCNC, TCNC/Cu NP (**b**), XRD patterns for CNC, Cu NP, TCNC (**c**) and TCNC/Cu NP synthesized with different ratios of TCNC/Cu NP (**d**)

Results and Discussion

Characterization of Modified Cellulose Nanocrystalline Loaded Copper Nanoparticles

Figure 2a displays the FTIR curves of CNC, TCNC and TCNC/Cu NP with different ratios. The absorption peak of –OH near 3418 $cm^{-1}$and the absorption peak of C–H near 2905 $cm^{-1}$are produced by stretching vibration. The peaks at 1430, 1372, and 1300 cm^{-1} correspond to the bending vibration peaks of $–CH_2$ and –OH groups. A new carboxyl peak (–COOH) appears at 1732 cm^{-1} in the spectrum of TCNC, indicating of a successful modification of CNC. In the TCNC/Cu NP spectrum, the –COOH peak at 1732 cm^{-1} is shifted to 1788 cm^{-1} because of the combination of –COOH and Cu^{2+}. The stretching vibration peak of the hydroxyl group moves to 3430 cm^{-1} with the introduction of –COOH [19]. Figure 2b exhibits the ultraviolet–visible (UV–Vis) absorption spectrums of CNC, TCNC, and TCNC/Cu NP with different ratios. It can be found that there is no absorption peak on the spectrums of CNC and TCNC. By contrast, all of TCNC/Cu NP nanohybrids could be examined with a characteristic peak in the region of 500–600 nm. As the increased ratio of Cu NP, the absorption peak intensity also increased obviously [20]. It is known that the absorption peak at 500–600 nm of TCNC/Cu NP is attributed to the surface plasmon resonance band of Cu NP, which demonstrates that Cu NP is formed during the formation of Cu NP in suspension.

Figure 2c exhibits the XRD patterns of CNC, TCNC, Cu NP, and various TCNC/Cu NP nanohybrids. As shown in Fig. 2c, the characteristic peaks of CNC occur at 16°, 22°

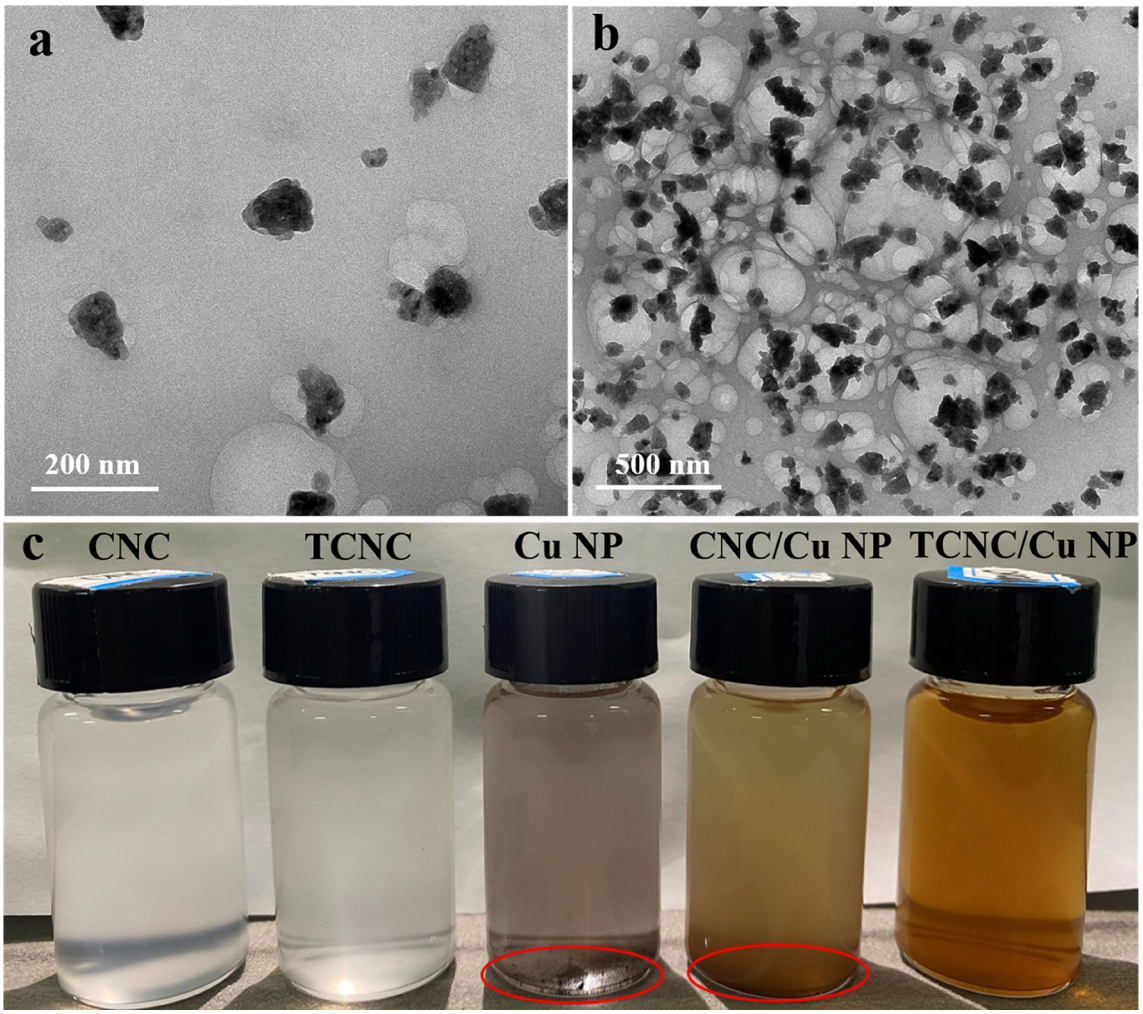

Fig. 3 TEM images of in the TCNC/Cu NP (1:1) nanocomposites (**a**, **b**) and graph of sedimentation experiment of CNC, TCNC, Cu NP, CNC/Cu NP and TCNC/Cu NP

and 34°, which are related to the (101), (002) and (040) crystal planes of the cellulose I-type crystal structure, respectively [21]. Although the carboxylation modification will cause minor damage of CNC, it still maintains high crystallinity. The peaks at 43.3°, 50.6°, and 74.3°, correspond to the (111), (200) and (220) crystal planes of nano copper, respectively. The peaks at 36.5° and 61.5° are the (111) and (113) crystal faces of CuO, respectively. The peak of 42.3° is the (220) crystal faces of Cu_2O. Figure 2d shows the XRD patterns of different TCNC/Cu NP nanohybrids, which can be ascribed to the diffraction of (111), (200) and (220) crystal planes of metallic copper crystals at 43.1°, 50.9°, and 74.1° [22]. These patterns prove the formation of Cu NP in the TCNC suspension. In addition, the peak at 36.5° is related to the crystal plane (111) of CuO owing to the slight oxidation of the Cu NP in the air.

Figure 3a and b show the TEM results of TCNC/Cu NP (1:1) nanohybrids. The modified carboxylic acid groups enable higher-density loading of Cu NP on the surface of TCNC, and the size distribution of TCNC/Cu NP (1:1) nanoparticles is about 40–80 nm [23]. Copper ions are adsorbed on TCNCs through electrostatic interaction and coordination, and grow in situ with TCNC as the nucleation site to form a well-structured nanohybrid.

The results of sedimentation experiment are shown in Fig. 3c, the pure Cu NP occurs obvious precipitation after standing for 2 h, while Cu NP loaded on CNC also precipitated at the bottom, demonstrating that only a part of Cu NP was fixed at the CNC. However, the dispersion of TCNC/Cu NP displays excellent stability after the carboxylation of CNC. The surface of the modified cellulose nanocrystals contains a large number of carboxyl groups and hydroxyl groups, so copper ions could be uniformly and tightly attached to the TCNC due to the presence of strong interaction. This interaction reduces the mobility of copper ions and stabilizes the Cu NP.

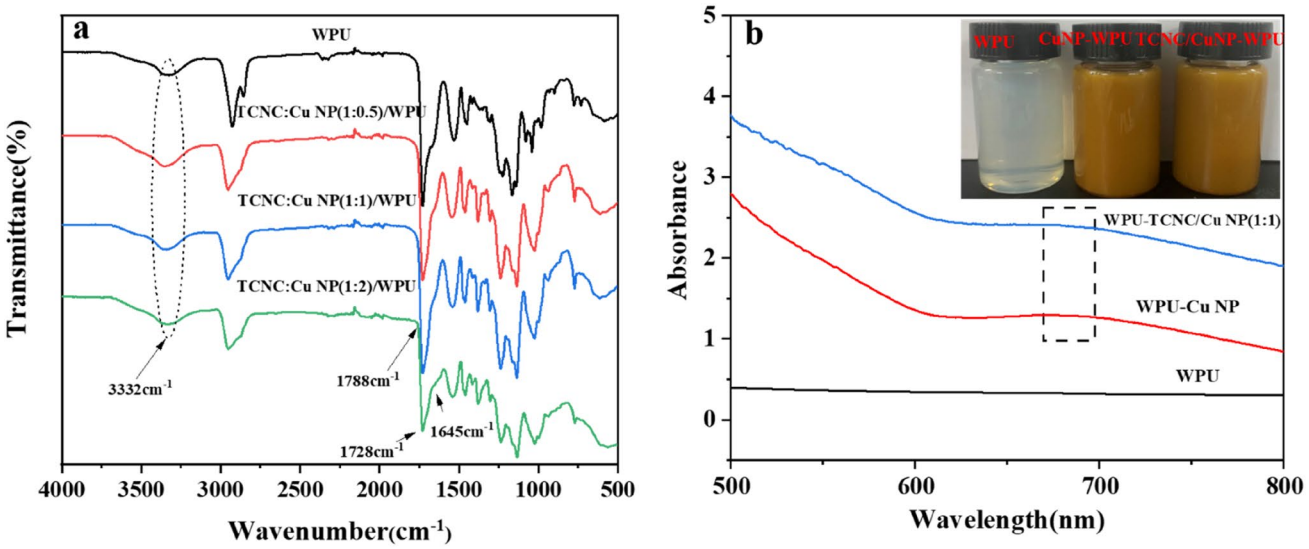

Fig. 4 ATR-FTIR curves of WPU film and different ratios of TCNC/Cu NP-WPU films (**a**) and UV–vis spectra of WPU, WPU-Cu NP, and WPU-TCNC/Cu NP

Composition and Surface Morphology of WPU and Various TCNC/Cu NP-WPU Nanocomposite Films

The ATR-FTIR curves of WPU and WPU nanocomposite films are shown in Fig. 4a [24]. The observed peak around 3332 cm^{-1} is related to the N–H stretching peak vibration of urethane. The peak at 1742 $cm^{-1}$of the pure WPU is attributed to the C=O stretching vibration of polyester polyol, and the peaks at 1145 and 1245 cm^{-1} belong to the vibration peaks of C–O–C in polyester, indicating of

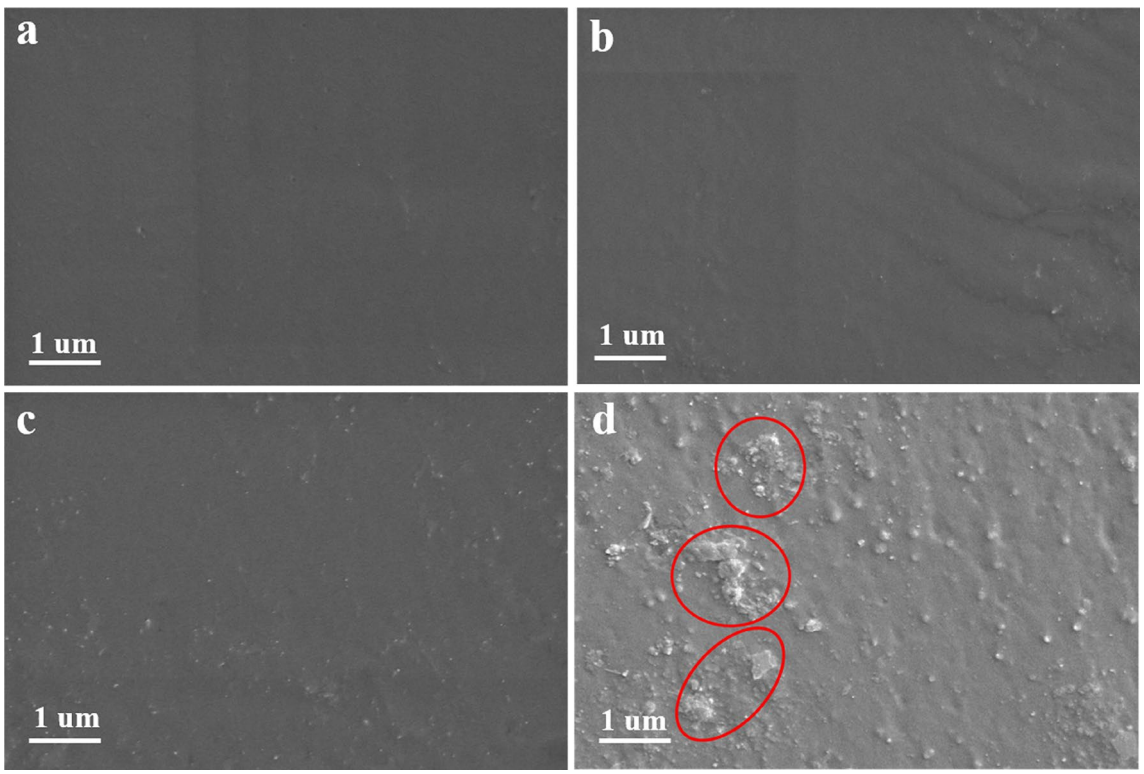

Fig. 5 SEM images of WPU film (**a**), TCNC/Cu NP (1:0.5)-WPU (**b**), TCNC/Cu NP(1:1)-WPU (**c**), TCNC/Cu NP (1:2)-WPU (**d**)

polyester type polyurethane. The band near 1645 cm^{-1} corresponds to the –OH of TCNC and the C=O group in the carbamate on the molecular chain of WPU. The strength of the peak decreases slightly with the continuous increase of TCNC/Cu NP, which may be due to the self-aggregation of excessive TCNC/Cu NP, thus hindering the interaction between the molecular chain of WPU and TCNC/Cu NP nanohybrids [25]. The UV absorption spectrums of different samples are shown in Fig. 4b. It can be found that a clear absorption band appears in the WPU dispersions with the addition of Cu NP and TCNC/Cu NP nanohybrids, which confirms the loading of metallic Cu NP on TCNC.

The fracture surface morphologies of the pure WPU film and WPU nanocomposite films loaded with different ratios of TCNC/Cu NP are displayed in Fig. 5 [26]. The fracture surface of the pure WPU film is relatively smooth, and white dots representing nanofillers can be clearly observed after adding TCNC/Cu NP (1:0.5) as shown in Fig. 5b. When the mass ratio of TCNC to $CuCl_2$ is 1:1(Fig. 5c), the nanohybrid particles are distributed uniformly on the fracture surface of TCNC/Cu NP (1:1)-WPU film. However, the fracture surface of TCNC/Cu NP (1:2)-WPU film has obvious agglomeration phenomenon and obvious pores with the increase of Cu NP content (Fig. 5d). The TCNCs have good dispersibility in the WPU matrix, and the dispersibility of copper nanoparticles is improved due to the effective combination of TCNCs with Cu NPs. However, too much copper content will agglomerate in the matrix, thereby affecting its performance [27].

The AFM images of WPU film and TCNC/Cu NP (1:1)-WPU film in 3D as shown in Fig. 6. The root mean square roughness (Rq) and average roughness (Ra) of WPU are 3.08 nm and 2.07 nm respectively, and the surface is flat. The Rq and Ra of WPU with TCNC/Cu NP (1:1) were 8.9 nm and 6.35 nm respectively. With the addition of TCNC/Cu NP composites, both Rq and Ra increase, and the surface roughness increases. The roughness difference between pure WPU and processed WPU can be observed in AFM image [28].

Mechanical, Scratch Resistance, and Thermal Properties

The mechanical property of WPU films is essential in practical applications. As shown in Fig. 7a, the tensile strength and modulus of the composite films with adding nanofillers increased first and then decreased. In comparison with the pure WPU film, the strength and modulus of WPU nanocomposite film incorporated with TCNC/Cu NP (1:1) increase from 15 and 66 MPa to 23 MPa and 134 MPa, separately. The significant improvement can be attributed to the expected stress transfer at the interface between TCNC/Cu NP and WPU thanks to the high aspect ratio of TCNC. Also, the hydrogen bond networks formed between –OH, –COOH groups of TCNC/Cu NP and –NH groups of WPU restrict the movement of WPU macromolecular chains, which enhances the strength [29]. For the TCNC/Cu NP (1:2)-WPU nanocomposite film, the mechanical properties decreased. This may be due to the lack of tight bonding of TCNC/Cu NP nanohybrids after the introduction of excess amount of copper nanoparticles [30].

As shown in Fig. 7c, the pencil hardness is used to characterize the scratch resistance of various samples. With increased ratio of Cu NP to TCNC, the pencil hardness of the WPU nanocomposite film added with TCNC/Cu NP (1:1) can reach 4H. The increased modulus appropriately avoids the phenomenon of stress concentration when the film is scratched [31]. With the further increased ratio of copper nanoparticles, the hardness of the composite film decreases, which is attributed to the agglomeration of copper

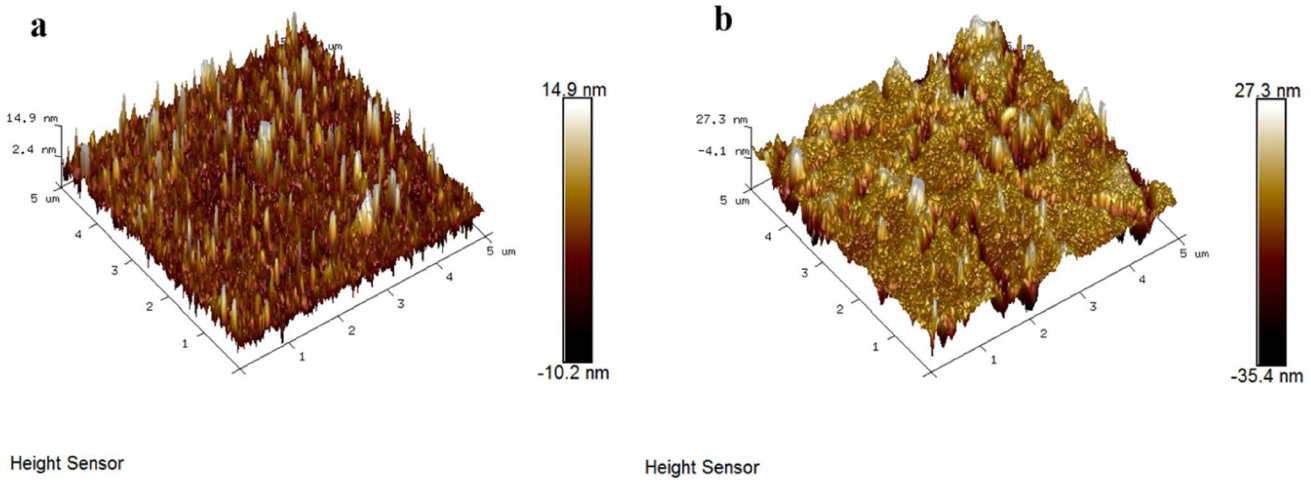

Fig. 6 AFM images of WPU film (**a**) and TCNC/Cu NP (1:1)-WPU film (**b**) in 3D

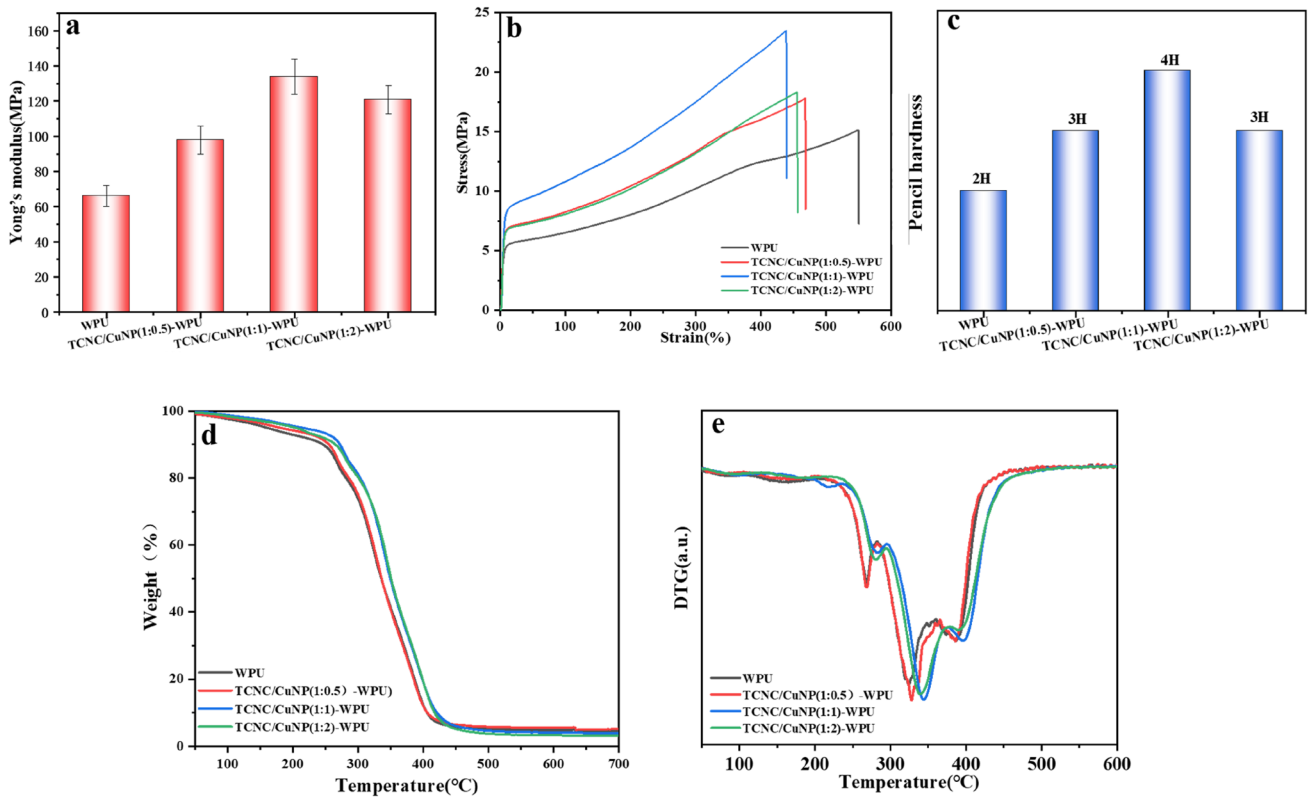

Fig. 7 Mechanical properties of WPU film and TCNC/Cu NP-WPU film (**a**–**c**) and TGA and DTG curves of the pure WPU film and TCNC/Cu NP-WPU film (**d**, **e**)

Table 1 Thermal analysis data of the pure WPU films and TCNC/Cu NP-WPU films

Samples	T10 (℃)	T50 (℃)
WPU	252	337
TCNC/Cu NP (1:0.5)-WPU	245	343
TCNC/Cu NP (1:1)-WPU	271	348
TCNC/Cu NP (1:2)-WPU	266	350

nanoparticles in WPU, thus destroying the structure of the composite film [32].

Figure 7d, e and Table 1 show thermogravimetric (TG) and derivative (DTG) curves of the pure WPU and WPU nanocomposite films. There are three obvious weight loss stages on the thermal weight loss curve of each sample, which is mainly because the structure of WPU is composed of different components. This finding shows that the modified WPU film and the pure WPU film exhibit similar thermal decomposition behavior at about 70℃–250℃. The weight loss stages at 250 °C–375°C and 375 °C–450°C correspond to the thermal decomposition of the hard and soft segment domains, respectively [33]. The DTG curve in Fig. 7d shows that the maximum weight loss temperature of WPU and TCNC/Cu NP-WPU is 324 ℃ and 345 ℃ respectively. In Table. 1, the T_{10} and T_{50} values of the pure WPU film are 246 °C and 335 °C, respectively. While the T_{10} and T_{50} of the WPU film with TCNC/Cu NP composites are shown in Table 1. These results indicate that the addition of TCNC/Cu NP composites remarkably improves the thermal stability of WPU. This condition may be due to the high crystallinity of TCNC and the strong interaction between the TCNC/Cu NP and WPU, which promote to formation of a three-dimensional network structure [34]. However, the addition of TCNC did not improve the thermal stability of the WPU soft segment, because the interaction between TCNC/Cu NPs and WPU was mainly formed in the hard segment micro-domains [35]. Therefore, the excellent thermal resistance of TCNC/Cu NP-WPU nanocomposite films may originate from the presence of Cu NP.

Antibacterial Activities

The antibacterial activities of all samples are evaluated using colony counting method. Two series of bacterial species are selected: *Escherichia coli* and *Staphylococcus aureus* (*Staphylococcus aureus*, as Gram-positive and *Escherichia coli*, as Gram-negative bacterial models, respectively).

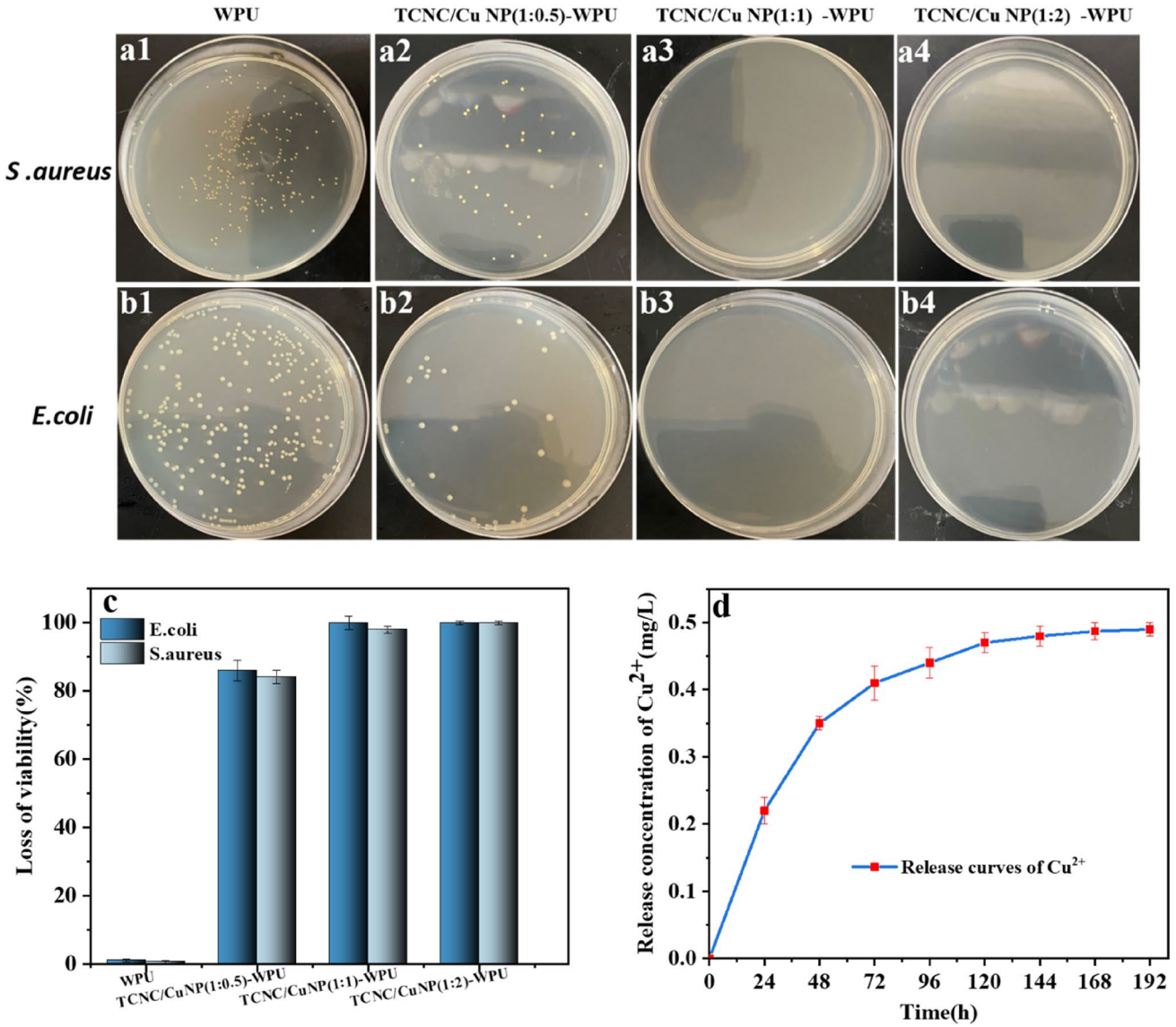

Fig. 8 Antibacterial properties of the films (**a** represents *S. aureus*; **b** represents *E. coli*; 1, 2,3, 4 represents WPU, TCNC/Cu NP (1:0.5)-WPU, TCNC/Cu NP (1:1-WPU) and TCNC/Cu NP (1:2)-WPU respectively. Bacteriostatic rate of WPU film and TCNC/Cu NP-WPU film (**c**) and Cu^{2+} release curve of TCNC/Cu NP (1:1)-WPU (**d**)

Figure 8 shows the results of the antibacterial test against *E. coli* and *S. aureus*. It can be concluded that a large number of bacteria adhere to the pure WPU film with no antibacterial activity. All of TCNC/Cu NP-WPU nanocomposite films exhibit good antibacterial properties and the specific data of antibacterial ratio is recorded in Fig. 8c. The presence of TCNC/Cu NP nanohybrids imparts composite films with good antibacterial properties that can be interpreted as the mechanism of copper ion release and contact with bacteria [36, 37]. In the case of TCNC/Cu NP (1:1), the antibacterial ratio against *E. coli* and *S. aureus* both reach 99.9%, indicating of outstanding antibacterial properties [38].

As depicted in Fig. 8d, the Cu^{2+} releasing behavior of the TCNC/Cu NP (1:1)-WPU film was analyzed by inductively coupled plasma optical emission spectrometer. In the release process of copper ion, the release amount in the first 24 h is 0.22 mg/L, and the release amount in 48 h is 0.35 mg/L. The release amount in 72, 96, 120, 144, 168 and 192 h were 0.410 mg/L, 0.440 mg/L, 0.470 mg/L, 0.480 mg/L, 0.487 mg/L and 0.490 mg/L respectively. The controlled release of copper ions is mainly due to the effective binding and loading of Cu NP on TCNC, which has good interfacial compatibility with the WPU matrix. Thus, the antibacterial agents of copper nanoparticles are firmly embedded in the

hydrogen bonding network structure formed, achieving a sustained release effect [39].

Conclusion

In summary, various WPU nanocomposite films incorporated with TCNC/Cu NP nanohybrids were fabricated via casting method. The AFM and SEM results show that the TCNC/Cu NP (1:1) nanohybrid is uniformly dispersed in the WPU matrix. hydrogen bond network is also formed between TCNC/Cu NP and the WPU matrix, resulting in improved mechanical, thermal and scratch resistant properties. Compared with the pure WPU film, the strength of TCNC/Cu NP-WPU increases by 53% (from 15 to 23 MPa), and the scratch resistance increases from 2 to 4H. Furthermore, The TCNC/Cu NP (1:1)—WPU nanocomposite films exhibit excellent antibacterial properties against E. coli and S. aureus. It is noteworthy that the nanocomposite film has a long-lasting antibacterial effect resulting from controlled release of copper ions. This work provides a feasible path to preparing the antibacterial WPU composite film.

Author Contribution XH: Methodology, Formal analysis, Software, Writing-original draft. YZ: Methodology, Formal analysis, Writing-original draft. YM: Methodology, Writing-review & editing. CS: Conceptualization, Resources, Writing–review & editing. JH: Conceptualization, Resources, Funding acquisition, Writing-review & editing.

Declarations

Competing Interest The authors declare that they have no known competing financial interests or personal relationships that could have appeared to influence the work reported in this paper.

References

1. Arantzazu S, Isabel F, Lorena U, Filomena B (2021) Green nanocomposites from Salvia-based waterborne polyurethane-urea dispersions reinforced with nanocellulose. Prog Org Coat 150:105989
2. Lu Y, Zhang P, Fan M, Jiang P (2019) Dual bond synergy enhancement to mechanical and thermal properties of castor oil-based waterborne polyurethane composites. Polymer 182:121832
3. Han G, Xiang Y, Zhu Y (2014) New Antibacterial composites: waterborne polyurethane/gold nanocomposites synthesized via self-emulsifying method. J Inorg Organomet 24:283–290
4. Fu H, Wang Y, Li X, Chen W (2016) Synthesis of vegetable oil-based waterborne polyurethane/silver-halloysite antibacterial nanocomposites. Compos Sci Technol 126:86–93
5. Zhang X, Wang W, Yu D (2018) Synthesis of waterborne polyurethane–silver nanoparticle antibacterial coating for synthetic leather. J Coat Technol Res 15:415–423
6. Zhang X, Zhu M, Wang W, Yu D (2018) Silver/waterborne polyurethane-acrylate's antibacterial coating on cotton fabric based on click reaction via ultraviolet radiation. Prog Org Coat 120:10–18
7. Sun C, Li Y, Li Z, Su Q, Wang Y, Liu X (2018) Durable and washable antibacterial copper nanoparticles bridged by surface grafting polymer brushes on cotton and polymeric materials. J Nanomater 212:876–879
8. Zhang Y, Liu B, Huang K (2020) Eco-friendly castor oil-based delivery system with sustained pesticide release and enhanced retention. ACS Appl Mater Inter 12:37607–37618
9. Miranda C, Llamazare R (2018) Cu nanoparticles/PVC composites: thermal, rheological, and antibacterial properties. Adv Polym Tech 37:937–942
10. Phana D, Dorjjugder N, Saito Y (2020) Muhammad Qamar Khand, antibacterial mechanisms of various copper species incorporated in polymeric nanofibers against bacteria. Mater Today Commun 25:101377
11. Feng H, Wang W, Wang T, Zhang L, Li W, Hou J (2023) Preparation of dynamic polyurethane networks with UV-triggered photothermal self-healing properties based on hydrogen and ion bonds for antibacterial applications. J Mater Sci Technol 133:89–101
12. Mirmohsenia A, Azizi M, Dorraji MS (2019) Facile synthesis of copper/reduced single layer graphene oxide as a multifunctional nanohybrid for simultaneous enhancement of antibacterial and antistatic properties of waterborne polyurethane coating. Prog Org Coat 131:322–332
13. Zhai J, Zhang Y, Cui C, Li A, Wang W, Guo R (2021) Flexible waterborne polyurethane/cellulose nanocrystal composite aerogels by integrating graphene and carbon nanotubes for a highly sensitive pressure sensor. ACS Sustain Chem Eng 9:14029–14039
14. Cheng D, Wei P, Zhang L (2019) New approach for the fabrication of carboxymethyl cellulose nanofibrils and the reinforcement effect in water-borne polyurethane. ACS Sustain Chem Eng 7:11850–11860
15. Mondragon G, Echart S, Hormaiztegui V (2018) Nanocomposites of waterborne polyurethane reinforced with cellulose nanocrystals from sisal fibres. J Polym Environ 26:1869–1880
16. Zhou Z, Lu C, Wu X, Zhang X (2013) Cellulose nanocrystals as a novel support for CuO nanoparticles catalysts: facile synthesis and their application to 4-nitrophenol reduction. RSC Adv 3:26066–26073
17. Pal N, Banerjee S, Roy P, Pal K (2021) Cellulose nanocrystals-silver nanoparticles-reduced graphene oxide-based hybrid PVA nanocomposites and its antimicrobial properties. Int J Biol Macromol 191:445–456
18. Fan X, Yu H, Wang D (2019) Facile and green synthesis of carboxylated cellulose nanocrystals as efficient adsorbents in wastewater treatments. ACS Sustain Chem Eng 7:18067–18075
19. Si R, Wu C, Yu D, Ding Q, Li R (2021) Novel TEMPO-oxidized cellulose nanofiber/polyvinyl alcohol/polyethyleneimine nanoparticles for Cu^{2+} removal in water. Cellulose 28:10999–11011
20. Wang T, Jian Z, Tang Q (2022) Interactions between atomically dispersed copper and phosphorous species are key for the hydrochlorination of acetylene. Chem Commun 5:1–10
21. Kwon G, Lee K, Kim D, Jeon Y, Kim U, You J (2020) Cellulose nanocrystal-coated TEMPO-oxidized cellulose nanofiber films for high performance all-cellulose nanocomposites. J Hazard Mater 398:123100
22. Phan D, Dorjjugder N, Saito Y, Khan M (2020) Antibacterial mechanisms of various copper species incorporated in polymeric nanofibers against bacteria. Mater Today Commun 25:101377
23. Liu H, Song J, Shang S (2012) Cellulose nanocrystal/silver nanoparticle composites as bifunctional nanofillers within waterborne polyurethane. ACS Appl Mater Inter 4:2413–2419
24. Liu R, Zhu F, Hu J (2021) Cellulose nanocrystals/water-based polyurethane nanocomposite films with excellent wear resistance and softness. Micro Nano Lett 16:268–273

25. Xi P, Wu L, Quan F, Xia Y, Fang K, Jiang Y (2022) Scalable nano building blocks of waterborne polyurethane and nanocellulose for tough and strong bioinspired nanocomposites by a self-healing and shape-retaining strategy. ACS Appl Mater Inter 19:675–678
26. Cheng Y, Wei Y, Fang C, Li H (2021) Facile synthesis of chitosan/Ag-waterborne polyurethane composite films with a high stability and controllable water resistance for potential application in antibacterial materials. J Mater Res Technol 15:5316–5325
27. Zhang Z, Se G, Wang X (2018) UV-absorbing cellulose nanocrystals as functional reinforcing fillers in poly (vinyl chloride) films. ACS Appl Nano Mater 1:632–641
28. Zhao S, Wang Z, Pang H, Zhang W, Zhang S (2019) Organic-inorganic nanohybrid polyurethane elastomer based on dopamine-mediated biomimetic co-deposition thought toward multiple improved properties. Appl Surf Sci 493:1340–1349
29. Wu G, Chen J, Huo S, Liu G, Kong Z (2014) Thermoset nanocomposites from two-component waterborne polyurethanes and cellulose whiskers. Carbohyd Polym 105:207–213
30. Wattanodorn Y, Jenkan R, Wirasate S (2014) Antibacterial anionic waterborne polyurethanes/Ag nanocomposites with enhanced mechanical properties. Polym test 40:163–169
31. Zhang H, She Y, Zheng X, Chen H, Pu J (2014) Optical and mechanical properties of polyurethane/surface-modified nanocrystalline cellulose composites. Chinese J Polym Sci 32:1363–1372
32. Li J, Hong R, Li M, Li H, Zheng Y, Ding J (2009) Effects of ZnO nanoparticles on the mechanical and antibacterial properties of polyurethane coatings. Prog Org Coat 64:504–509
33. Xu J, Li T, Zhao W, Li P, Wu Y (2016) Synthesis and characterization of waterborne polyurethane emulsions based on poly (butylene itaconate) ester. Des Monomers Polym 19:309–318
34. Liu S, Zhao B, Jiang L, Zhu Y (2018) Core–shell Cu@ rGO hybrids filled in epoxy composites with high thermal conduction. J Mater Chem C 6:257–265
35. Yang F, Wu Y, Zhang S, Zhang H, Zhao S (2020) Mechanical and thermal properties of waterborne polyurethane coating modified through one-step cellulose nanocrystals/graphene materials sols method. Coatings 10:40
36. Chatterjee A, Chakraborty R, Basu T (2014) Mechanism of antibacterial activity of copper nanoparticles. Nanotechnology 25:135101
37. Ma W, Soroush A, Luong T, Rahaman M (2017) Cysteamine- and graphene oxide-mediated copper nanoparticle decoration on reverse osmosis membrane for enhanced anti-microbial performance. J Colloid Interf Sci 501:330–340
38. Mirmohseni A, Azizi M, Dorra S (2019) A promising ternary nanohybrid of Copper@ Zinc oxide intercalated with polyaniline for simultaneous antistatic and antibacterial applications. J Coat Technol Res 16:1411–1422
39. Kim Y, Min B (2017) Preparation of bio-polyurethane using castor oil and antibacterial hybrid films thereof with silver-doped hydroxyapatite. Fiber Polym 18:1841–1847